

ORIGINAL ARTICLE

Molecular Genetic Analysis of p53 Intratumoral Heterogeneity in Human Astrocytic Brain Tumors

Zhi-Ping Ren, MD, PhD, Tommie Olofsson, MD, Mingqi Qu, MD, PhD, Göran Hesselager, MD, PhD, Thierry Soussi, PhD, Hannu Kalimo, MD, PhD, Anja Smits, MD, PhD, and Monica Nistér, MD, PhD

Abstract

We investigated genetic heterogeneity of astrocytic gliomas using p53 gene mutations as a marker. Different parts of morphologically heterogeneous astrocytic gliomas were microdissected, and direct DNA sequencing of p53 gene exons 5 through 8 was performed. Thirty-five glioma samples and tumor-adjacent normal-appearing brain tissue from 11 patients were analyzed. Sixteen different p53 gene mutations were found in 7 patients. We found that some tumors were devoid of p53 gene mutations, whereas other tumors carried 1 or often several (up to 3) different mutations. The mutations were present in grade II, III, and IV astrocytic glioma areas. Both severe functionally dead mutants and mutants with remaining transcriptional activity could be observed in the same tumor. We observed that morphologically different parts of a glioma could carry different or similar mutations in the p53 gene and could be either associated or not associated with the locus of heterozygosity at the mutant site. Coexistence of p53 gene mutations and the locus of heterozygosity was common, at least in astrocytomas grade III and in glioblastomas, and also occurred in astrocytoma grade II areas. These results support the notion that intratumoral heterogeneity in brain tumors originates from different molecular defects. Our results are of importance for a further understanding of the molecular mechanisms behind failure to treat glioma patients.

Key Words: Clonality, Glioma, Heterogeneity, Microdissection, Mutation, p53.

INTRODUCTION

Astrocytic tumors are the most common primary tumors evolving in the brain (1). A characteristic feature of most astrocytic tumors is the combination of various genetic aberrations, leading to both inactivation of tumor suppressor genes and amplification of oncogenes. Gliomas in general and astrocytic tumors in particular are relatively resistant to standard oncologic treatment such as radiotherapy and chemotherapy. However, subgroups of patients may exist that benefit from treatment, even among the most malignant forms of gliomas (2). Currently, the estimation of prognosis and choice of therapy are to a large extent based on neuropathologic diagnosis of samples removed by needle biopsies or open surgery. Thus, clinical management of astrocytic tumors relies on accurate histopathologic diagnosis of malignancy grade and subtype of tumor according to the criteria given in the World Health Organization classification of tumors of the nervous system (3) and routine histologic staining methods and immunohistochemistry of formalin-fixed, paraffin-embedded material. In addition to histopathologic diagnosis, molecular genetic classification of different gliomas is becoming more and more important for the comprehensive definite diagnosis and clinical management (4).

The p53 gene is commonly mutated in astrocytic gliomas (5). Clinically, 2 types of glioblastomas are defined: primary and secondary glioblastomas. Primary glioblastomas arise de novo and manifest rapidly without evidence of a less malignant precursor lesion. They account for the vast majority of cases in older people and are genetically characterized by a high frequency of epidermal growth factor receptor (*EGFR*) gene amplification. The secondary glioblastomas develop more slowly by progression from a low-grade astrocytoma. They typically occur in younger patients and about two thirds of the tumors have mutations in the p53 gene, which is also the most common aberrant gene in grade II and grade III astrocytomas. Approximately 50% of these tumors have no wild-type p53 gene, and a further 10% to 15% have 1 wild-type and 1 mutated allele (6, 7). Of all the p53 gene mutations identified in low-grade glioma, 90% were located at CpG sites, suggesting a common mechanism of acquisition of these mutations in low-grade gliomas. Furthermore, in low-grade gliomas identified in a population-based study, approximately 60% of the p53 gene mutations were clustered in 2 hot spot codons, that is, codons 248 and 273 (8). In primary glioblastomas, p53 gene mutations were found in only about 30% of the tumors, and

From the Department of Genetics and Pathology (Z-PR, TO, HK), Department of Neuroscience (MQ, GH, AS), Uppsala University, University Hospital, Uppsala, Sweden; Department of Oncology Pathology (MQ, TS, MN), Karolinska Institutet, Karolinska University Hospital, Stockholm, Sweden; Department of Neurosurgery (MQ), West China Hospital, Sichuan University, China; Université P.M. Curie (TS), Paris 6, Paris, France; and Department of Pathology (HK), University Hospital of Helsinki, Helsinki, Finland.

Send correspondence and reprint requests to: Anja Smits, MD, PhD, Department of Neuroscience, Neurology, University Hospital Uppsala, S-751 85 Uppsala, Sweden; E-mail: Anja.Smits@neurologi.uu.se

Drs. Ren and Olofsson contributed equally to this work.

This work was supported financially by grants from the Swedish Cancer Foundation (Z-PR, MN), the Selanders Research Fund (AS) and the Lions Cancer Research Fund at Uppsala University Hospital (Z-PR, AS), and the Cancer Society in Stockholm (MN).

a more widespread distribution of mutations over the p53 gene was seen rather than a clustering in hot spots.

The histologic intratumoral heterogeneity of gliomas is well recognized, whereas knowledge of the relationship between histologic and molecular genetic heterogeneity is still fragmentary; that is, whether the genetic alterations are present in any sample of a tumor or whether only some regions with specific histologic phenotype bear the aberrations (9). With systematic and detailed molecular analysis of regional heterogeneity in a tumor we may learn more about the origin of the tumor cells. Identification of subsets of tumor cells within the tumor-bearing genetic aberrations with prognostic value may be important in the clinical management of patients with certain gliomas for which minimal invasive surgery and stereotactic biopsies are often used.

In this study we examined a series of astrocytic gliomas from 11 patients by microdissecting multiple samples from the tumors and analyzing p53 gene mutations in the dissected cell populations. We describe the presence of different p53 gene mutations in direct correlation to histologic characteristics of the dissected tumor areas.

MATERIALS AND METHODS

Glioma Samples

Eleven glioma samples, consisting of astrocytic tumors of different grades of malignancy, were obtained from 11 patients whose gliomas were diagnosed at the Department of Genetics and Pathology, Uppsala University Hospital, Uppsala, Sweden. Seven male and 4 female patients aged from 22 to 69 years were included (Table 1). Histopathologic diagnoses were reevaluated for the purpose of this study. All samples were multiply microdissected. All selected slides were then carefully rereviewed (including use of additional immunohistochemical stainings when needed) by 2 neuropathologists (T.O. and H.K.) to classify

the histopathology of the different areas to be microdissected and graded according to the World Health Organization criteria (1). Tumors with components resembling oligodendroglioma were excluded from the study.

Microdissection and DNA Preparation

All samples were formaldehyde-fixed and paraffin-embedded tissues. Microdissection and DNA preparation were performed as described (10, 11) with some modification for fixed and paraffin-embedded tissue (12). Paraffin-embedded blocks were consecutively sectioned, and sections were stained with hematoxylin and eosin. Areas with different histopathology were identified and marked on the hematoxylin and eosin-stained slides by the neuropathologists. These marked slides served as a guide map for microdissection and for histopathologic diagnosis of the different tumor areas. In all of the astrocytic tumors from 11 patients, multiple areas were microdissected. In 8 cases, morphologically normal surrounding brain tissue was included in the material and separately microdissected.

For microdissection, 10- μ m-thick paraffin sections were dissected with a small scalpel under light microscopy. The scalpel was changed after each dissection. The dissected material from consecutive sections was pooled in Eppendorf tubes containing 100 μ L of buffer (10 mM Tris-HCl, pH 8.0; 1 mM EDTA, and 1% Tween 20) and 2 to 8 μ L of proteinase K (20 μ g/ μ L). Cells were lysed overnight at 56°C. The cell lysates were heated for 10 minutes at 95°C to inactivate the proteinase K. The Eppendorf tubes were centrifuged at 14,000 rpm for 10 minutes before the supernatant was used as a DNA template for running polymerase chain reaction (PCR).

Oligonucleotides and Thermocycling

All p53 gene-specific primers were obtained from DNA Technology (Aarhus, Denmark). Four pairs of primers

TABLE 1. Clinical Data from the 11 Patients With Glioma Showing Diagnosis, Number of Dissected Samples, Distance Between Dissected Samples, Sex, Age of the Patient at Diagnosis and at Operation, and Tumor Localization

Case	Clinical Diagnosis	No. of Dissected Samples	Approx. Distance Between Dissected Areas	Sex	Age at Diagnosis/ at Operation	Tumor Localization/Side
1	GB	3	From 3 separate pieces of 2 paraffin blocks	M	61/61	Frontotemporal/L
2	GB	4	1 mm between normal brain and AIII; GB on separate piece of the same block	M	50/50	Frontotemporal/R
3	GB	3	2 mm between AII and GB; another GB is on separate piece of the same block	F	43/43	Parietal/L
4	GB	4	4 mm between normal brain and 2 GBs which were 1 mm from each other; the other GB on different block	M	77/77	Temporal/L
5	GB	5	From separate pieces of 4 paraffin blocks	M	43/57	Parietal/R
9	AII	2	0 mm between normal area and AII	M	40/41	Frontotemporal/L
10	AII	2	From separate pieces of the same paraffin block	M	50/51	Frontotemporal/L
11	GB	3	From 3 separate pieces of 2 paraffin blocks	F	69/69	Frontotemporal/L
12	GB	3	1mm between normal brain and GB; the other GB on separate piece of the same block	F	59/59	Frontal/R
13	GB	3	5, 7, and 2 mm	F	68/68	Frontal/L
15	AIII	3	0 mm between normal brain and AII; AIII on separate block	M	47/48	Frontal/R

GB, glioblastoma; AII, astrocytoma grade II; AIII, astrocytoma grade III; M, male; F, female; L, left; R, right.

were used for p53 gene fragment amplification, which included exons 5 through 8. The sequences of these primers are exon 5, 5'-TTC CTC TTC CTA CAG TAC TC-3', 5'-AGC TGC TCA CCA TCG CTA TC-3'; exon 6, 5'-CAC TGA TTG CTC TTA GGT CTG-3', 5'-AGT TGC AAA CCA GAC CTC-3'; exon 7, 5'-GTG TTA TCT CCT AGG TTG GC-3', 5'-AAG TGG CTC CTG ACC TGG AG-3'; and exon 8, 5'-TTC CTA TCC TGA GTA GTG G-3', 5'-CTT CTT GTC CTG CTT GCT TAC-3'. The PCR-amplified fragment lengths are exon 5, 209 base pairs (bp); exon 6, 129 bp; exon 7, 138 bp; and exon 8, 174 bp. Thermocycling was modified from previously reported methodology (13). Briefly, PCR reactions were carried out in GeneAmp PCR System 9600 (PerkinElmer Life and Analytical Sciences, Norwalk, CT) and a GeneAmp PCR System 2700 thermocycler (Applied Biosystems, Foster City, CA) using a mixture (20 μ L) containing the DNA extracted from the different cell lysates, 10 mM Tris-HCl (pH 8.3), 2 mM MgCl₂, 50 mM KCl, 0.1% Tween 20, 0.2 mM dNTP; 10 mM concentrations of each primer, and 0.5 unit of platinum Taq DNA Polymerase (Invitrogen, Carlsbad, CA). Temperature cycles and times for PCR reactions were denaturation at 94°C for 30 seconds, annealing at 55°C for 30 seconds, and extension at 72°C for 30 seconds. Each PCR reaction was preceded by a 3-minute denaturation at 94°C, and the final cycle was followed by a 7-minute extension at 72°C. The total number of cycles for PCR amplification was 40 to 45, depending on the sample DNA.

Purification of PCR Product and Sequencing

All PCR products were purified before sequencing reaction by enzymatic purification method. Six microliters of PCR products were mixed with 1 μ L of Exonuclease I (10 unit/ μ L) and 1 μ L of shrimp alkaline phosphatase (1 unit/ μ L) (Amersham-Pharmacia Biotech, Uppsala, Sweden). The mixture was placed on a GeneAmp PCR System 2700 thermocycler at 37°C for 30 minutes to digest the single strand nucleotide and at 80°C for 20 minutes to inactivate the enzyme. An ABI Prism BigDye Terminator Cycle Sequencing Ready Reaction Kit (Applied Biosystems) was used for the sequencing of PCR products. Automatic sequencing was performed with ABI 377 and ABI 310 DNA sequencers (Applied Biosystems).

Sequences were analyzed from both strands to validate laboratory findings. When a mutation was observed in 1 strand we confirmed its presence by sequencing the other strand of the same PCR products. In addition, we also confirmed the mutations identified by reanalyzing the original DNA template using another set of primers for exon 5 through 8 of the p53 gene (14). To define a mutation we analyzed each nucleotide peak by using the Sequencher program (version 4.1.2; Gene Codes Corporation, Ann Arbor, MI). The detection limit for mutations was set to 15% signal over noise at polymorphic positions (15).

Loss of Heterozygosity

We did not have access to normal DNA from patient's blood to perform microsatellite markers of the p53 gene region. Therefore the criteria for loss of heterozygosity

(LOH) were based on the proportion of mutation signal peak size over wild-type signal peak size at the same sequencing site (16). We set a high restriction for determination of LOH status in the samples. The defined LOH was set to 90% mutation signal over the wild-type signal at the polymorphic positions.

p53 Immunohistochemistry

p53 protein expression was detected on 5- μ m formaldehyde-fixed, paraffin-embedded sections from the same blocks used for microdissection. Paraffin-embedded blocks were consecutively sectioned, and the microdissected areas were analyzed for immunoreactivity by using a monoclonal IgG2b mouse anti-human p53 antibody M7001 (Dako, Glostrup, Denmark). The recommendations of the manufacturer were followed for immunostaining procedures. Immunoreactivity (IR) was scored on a scale of “-” to “3+”, as assessed by a single neuropathologist (T.O.) as follows: -, no (0%) p53-IR cells; 1+, low number (\leq 33%) of p53-IR cells; 2+, moderate number ($>$ 33% but \leq 66%) of p53-IR cells; and 3+, high number ($>$ 66%) of p53-IR cells. “2+” and “3+” were taken to represent overexpression of p53 protein.

Analysis of p53 Gene Mutation Frequency and Functional Effects

Analysis of p53 gene mutation frequency was performed using the last release of the UMD p53 database (release 2007_R1b, <http://p53.free.fr>) that includes 26,000 p53 gene mutations (17). This release contains the functional activity of all mutant p53 as tested in a yeast transcription assay by Kato et al (18). Briefly, haploid yeast transformants containing p53 gene mutations and a green fluorescent protein reporter plasmid have been constructed. p53 mutant activity was tested by measuring the fluorescent intensity of green fluorescent protein that is controlled by the various promoter sequences of the plasmid after 3 days of growth at 37°C (18).

RESULTS

Altogether, 35 astrocytic glioma samples, including morphologically normal brain tissue adjacent to the tumor, from 11 patients were collected. The diagnoses were classified according to the World Health Organization and included 2 cases of astrocytoma grade II (AII), 1 case of astrocytoma grade III (AIII), and 8 cases of glioblastoma (GB) (Table 1). All tumors were multiply microdissected and because the tumors were heterogeneous, morphologically different parts (including different grades of malignancy) were sampled. The approximate distance between the dissected areas was estimated except for those cases in which microdissections were performed on separate blocks (Table 1). Initially, the list included a few additional tumors that were excluded because of the presence of oligodendroglioma components or the shortage of material (Table 1).

p53 Gene Mutations and LOH, and p53 Protein Accumulation

Sixteen p53 gene mutations were found in 14 glioma samples from 7 of 11 patients. Fourteen were missense

mutations, causing amino acid transition (9 variants), 1 was a silent mutation, and 1 was a deletion causing a frameshift. Three occurred on hot spot codons for gliomas (1 in 248, 2 in 282) (3). In 13 glioma samples from 6 patients only wild type p53 was detected. Four of the 11 tumors (all GBs) were wild type for p53 in all microdissected areas. The primary data are summarized in Table 2.

Mutations in the p53 gene within multiple samples from the same tumor were observed in 6 of 7 tumors with mutations (cases 1, 2, 4, 5, 9, and 15). These mutations were distributed in different ways in the microdissected areas. For example, 2 different mutations coexisted in both microdissected cell populations of case 2 (codons 164 and 234 and 128 and 234). In other cases, different mutations were associated with different malignancy grades (cases 1 and

15). On 3 occasions, microdissected samples from different areas of the same tumor with either different malignancy grades (case 5) or different morphologies (cases 2 and 9) shared an identical mutation. For several cases, the microdissected areas containing p53 gene mutations showed the coexistence of positive immunostaining for the p53 protein (Table 2). Overexpression of the p53 protein was only found in a number of microdissected areas with morphology of high-grade glioma. Because immunohistochemistry was performed in a later phase of the study, consecutive sections of microdissected areas could not be recovered for all cases, and no results were obtained for these cases (cases 3, 9, 11, and 12).

Three patients with GBs (cases 11–13) had wild-type p53 exons 5 through 8, as frequently reported in primary

TABLE 2. Primary Data From All 11 Cases With Number of Microdissected Samples, Mutation Signals From Forward and Reverse Strand Sequencing, Estimated LOH Status, and TP53 IHC Status

Case	Histologic Diagnosis	Identified Areas	Mutated Codons and Exons	Signal Mutation/wt (%)	LOH	TP53 IHC Status
1	GB	Normal	wt			Negative
1		AII	140: exon 5	F 100%; R 100%	Positive	Negative
1		GB	282: exon 8	F 75%; R 60%	Negative	Positive +
2	GB	Normal 1	wt			Negative
2		Normal 2	wt			Negative
2		AIII	164: exon 5, 234: exon 7	164: F 50%; R 75%; 234: R 100%	164: negative; 234: positive	Positive ++
2		GB	128: exon 5, 234: exon 7	128: R100%; 234: R 100%	Positive	Negative
3	GB	AII	wt			NA
3		GB	wt			NA
3		GB	wt			NA
4	GB	Normal	wt			Negative
4		GB	wt			Negative
4		GB	280: exon 8	F 100%; R 100%	Positive	Negative
4		GB	178: exon 5, deletion C	F 100%; R 100%	Positive	Negative
5	GB	Normal	149: exon 5	F 50%; R 50%	Negative	Negative
5		AII	134: exon 5	F 100%; R 90%	Positive	Negative
5		AII	wt			Negative
5		GB	134: exon 5	F 100%; R 100%	Positive	Positive ++
5		GB	134: exon 5	F 100%	Positive	Positive ++
9	AII	AII	134: exon 5	F 20%; R 25%	Negative	NA
9		AII	134: exon 5	R 80%	Negative	NA
10	AII	Normal	wt			Negative
10		AII	248: exon 7	F 100%; R 100%	Positive	Positive+
11	GB	GB	wt			NA
11		GB	wt			NA
11		GB	wt			NA
12	GB	Normal	wt			NA
12		GB	wt			NA
12		GB	wt			NA
13	GB	GB	wt			(+)
13		GB	wt			(+)
13		GB	wt			(+)
15	AIII	Normal	wt			Negative
15		AII	137: exon 5	F 30%; R 40%	Negative	Negative
15		AIII	282: exon 8	F 95%; R 100%	Positive	Positive ++

GB, glioblastoma; wt, wild type; AII, astrocytoma grade II; AIII, astrocytoma grade III; LOH, loss of heterozygosity; F, forward; R, reverse; IHC, immunohistochemistry; NA, not applicable.

GB. In another patient with a GB (case 3) with an adjacent AII region, the whole tumor similarly harbored wild-type p53.

Eight areas from 7 patients could be microdissected from morphologically normal-appearing brain tissue adjacent to the tumor. Only 1 of these areas showed a mutation in the p53 gene (case 5). This was a silent mutation, different from the functionally compromised mutation in the tumor.

Comprehensive descriptions of individual cases are given in the legends of Figures 1 through 5, which illustrate the various relations observed between histopathology, p53 gene mutations and LOH, and p53 immunoreactivity (Table 2). Schematic drawings of glioma samples micro-

dissected from different morphologically defined areas are presented, with corresponding information on p53 gene mutations and estimated LOH status. The 7 multiply sampled gliomas in which p53 gene mutations were recorded are illustrated. The microscopic pictures of the tumor parts are representative of the tissues in the microdissected areas. The figures also include a functional evaluation of each identified mutation (19), with specific mutations illustrated.

Tables 1 and 2 show the various characteristics of the observed p53 gene mutations using the last version of the UMD p53 database as discussed above. The functional consequences of the mutation for transcription activity are

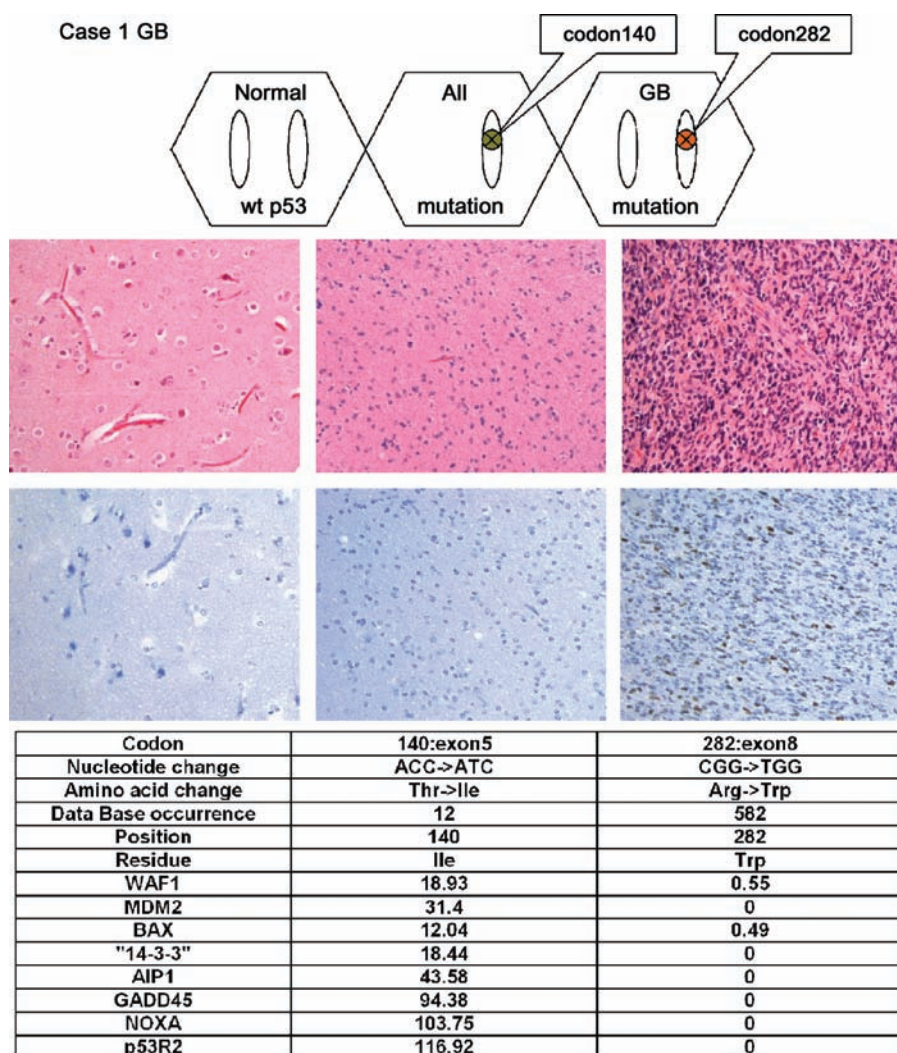


FIGURE 1. Case 1. Glioblastoma (GB). Three microdissected samples were taken from morphologically normal brain adjacent to tumor (left micrograph), astrocytoma grade II (AII) (middle micrograph) and GB (right micrograph). Each hexagon represents 1 microdissected cell population. Each unfilled elliptic bar represents 1 p53 allele in the group of cells. The small circle with a cross represents a missense mutation. Normal-appearing brain cells showed wild-type (wt) p53. Two missense mutations were observed in the tumor. One was found in the AII portion and the other, a hot spot mutation in codon 282, was observed in the GB area. This mutant is functionally "dead," whereas the codon 140 mutation in the AII area is "mild." One p53 allele was lost in the AII part of the glioma, suggesting that the 2 cell populations had followed their own alternative pathways in tumor progression. Both the AII and GB parts had lost the function of 1 allele but via different mechanisms. Immunostaining revealed a low level of p53-immunoreactivity (IR) in the GB area, but no p53-IR in the normal brain and AII area.

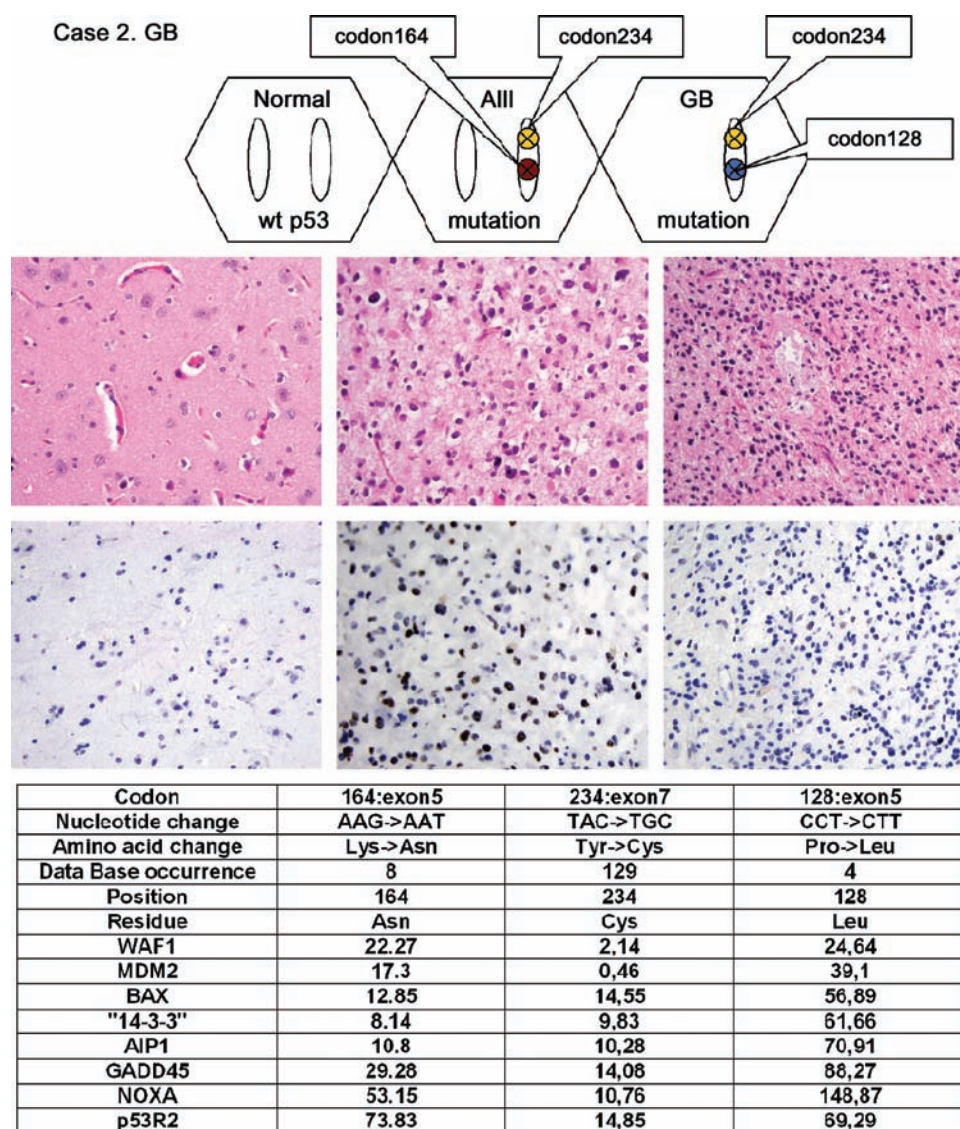


FIGURE 2. Case 2. Glioblastoma (GB). Three samples were obtained including normal-appearing brain, astrocytoma grade III (AIII) and GB. Each hexagon represents 1 microdissected cell population. Each unfilled elliptic bar represents 1 p53 allele in the group of cells. The small circle with a cross represents a missense mutation. Three different missense mutations were found, distributed as 2 pairs having in common the mutation in codon 234, which encoded a protein with low functional activity, whereas the 2 other mutations were milder. p53 protein overexpression was found in the AIII area, whereas the normal brain and GB showed negative or very low immunoreactivity. Note that the 2 mutations in the middle hexagon can exist in 1 allele or in separate alleles and in separate cells because the DNA analyzed is collected from a pool of cells. In the AIII area shown to the right, 1 p53 allele was lost. wt, wild-type.

given for 8 p53 target gene promoters associated with various effects of p53, such as growth arrest (WAF1 and 14-3-3), DNA repair (GADD45 and P53R2), apoptosis (BAX, AIP1, and NOXA), and p53 regulation (MDM2). Data are provided by the UMD p53 database and are taken from the work of Kato et al (18, 19). p53 activity was analyzed in a yeast assay, and data indicated here correspond to the percentage of remaining activity of mutant p53 compared with wild-type p53 (100%). For each mutant the frequency of occurrence in the database is given. Mutants found more

than 50 times are usually considered as hot spot mutations and are always deleterious for p53 activity.

The LOH for p53 gene exons 5 to 8 was estimated on the basis of the proportion of mutation signal peak size over the wild-type signal peak size at the sequencing site; therefore, we could only observe LOH in cases/areas with mutations. LOH was a common finding and coexisted with a mutation in 6 of 7 cases (1 AII, 1 AIII, and 4 GBs). The evaluation was difficult for the other AII that was included in the study.

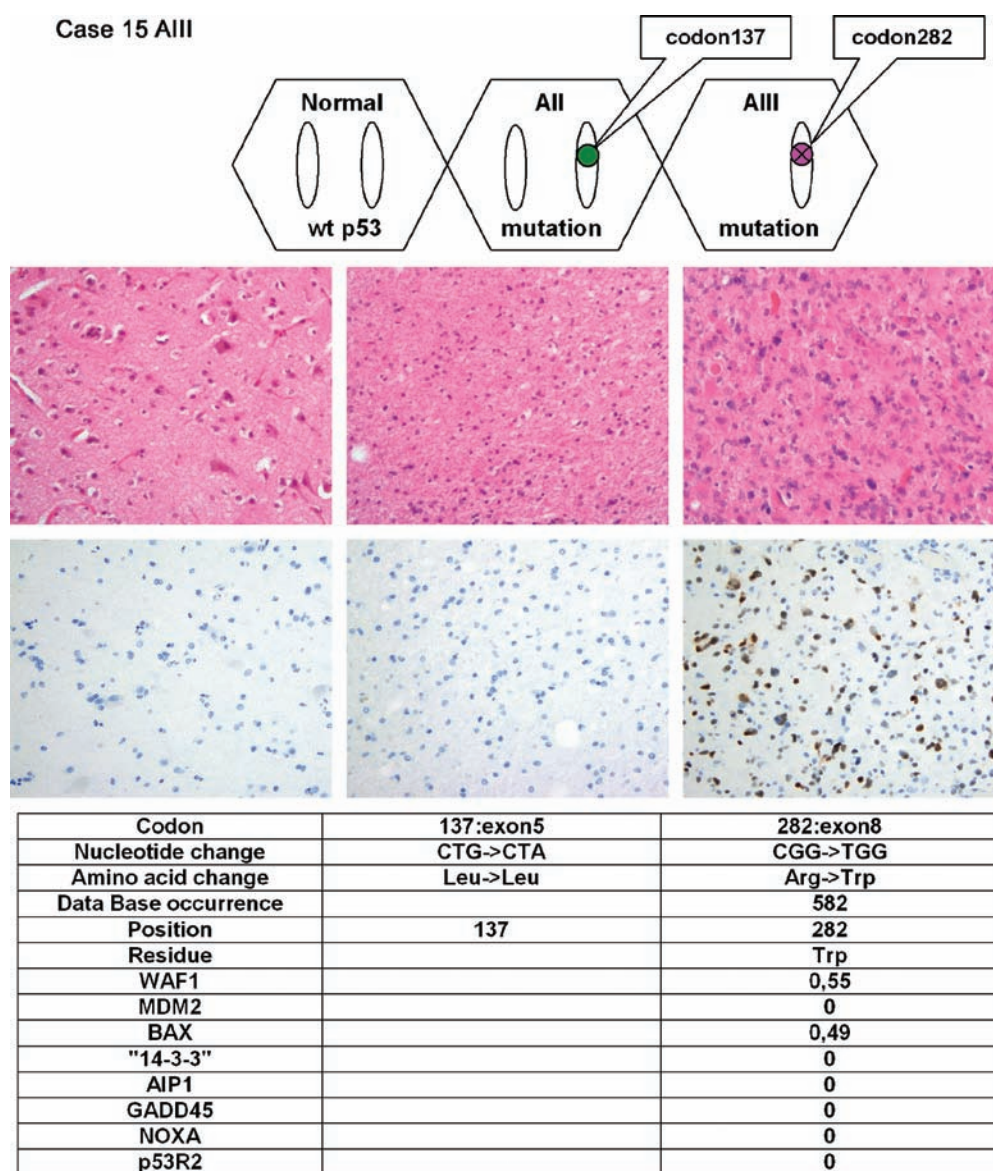


FIGURE 3. Case 15. Astrocytoma grade III (AIII). Three areas were microdissected and different mutations were found in the astrocytoma grade II (AII) and AIII area. Each hexagon represents 1 microdissected cell population. Each unfilled elliptic bar represents 1 p53 allele in the group of cells. The small circle with a cross represents a missense mutation. The codon 282 mutation in the AIII area was a hot spot mutation, which totally disrupted the function of the encoded p53 protein, whereas the codon 137 mutation in the AII part was a silent mutation without amino acid change. In addition, 1 allele was clearly lost in the AIII area. Immunostaining revealed overexpression of p53 protein in the AIII area, but no p53-immunoreactivity in the normal brain and AII area. wt, wild-type.

From the above-described p53 mutation analyses of different microdissected areas, we conclude that 1 of 8 normal areas, 6 of 8 AII areas, 2 of 2 AIII areas, and 6 of 11 GB areas harbored p53 mutations. LOH was observed in 0 of 1 of the normal area, 3 of 6 of the AII areas, 2 of 2 of the AIII areas, and 5 of 6 of the GB areas carrying p53 mutations.

DISCUSSION

The primary objective of this study was to gain further insight into the molecular genetic heterogeneity of astrocytic

gliomas. p53 gene mutations were used as a genetic marker for intratumoral heterogeneity. Therefore, we microdissected morphologically different areas within the tumor and studied the p53 status in these areas by direct DNA sequencing of p53 exons 5 through 8. We found heterogeneity of p53 gene mutations within 5 of the 11 astrocytic gliomas, of which many mutations had significant functional consequences. This study may shed light on the functional involvement of p53 gene mutations at an early stage of glioma development.

Molecular analysis of genomic DNA extracted from paraffin tissue can generate PCR artefacts that can be

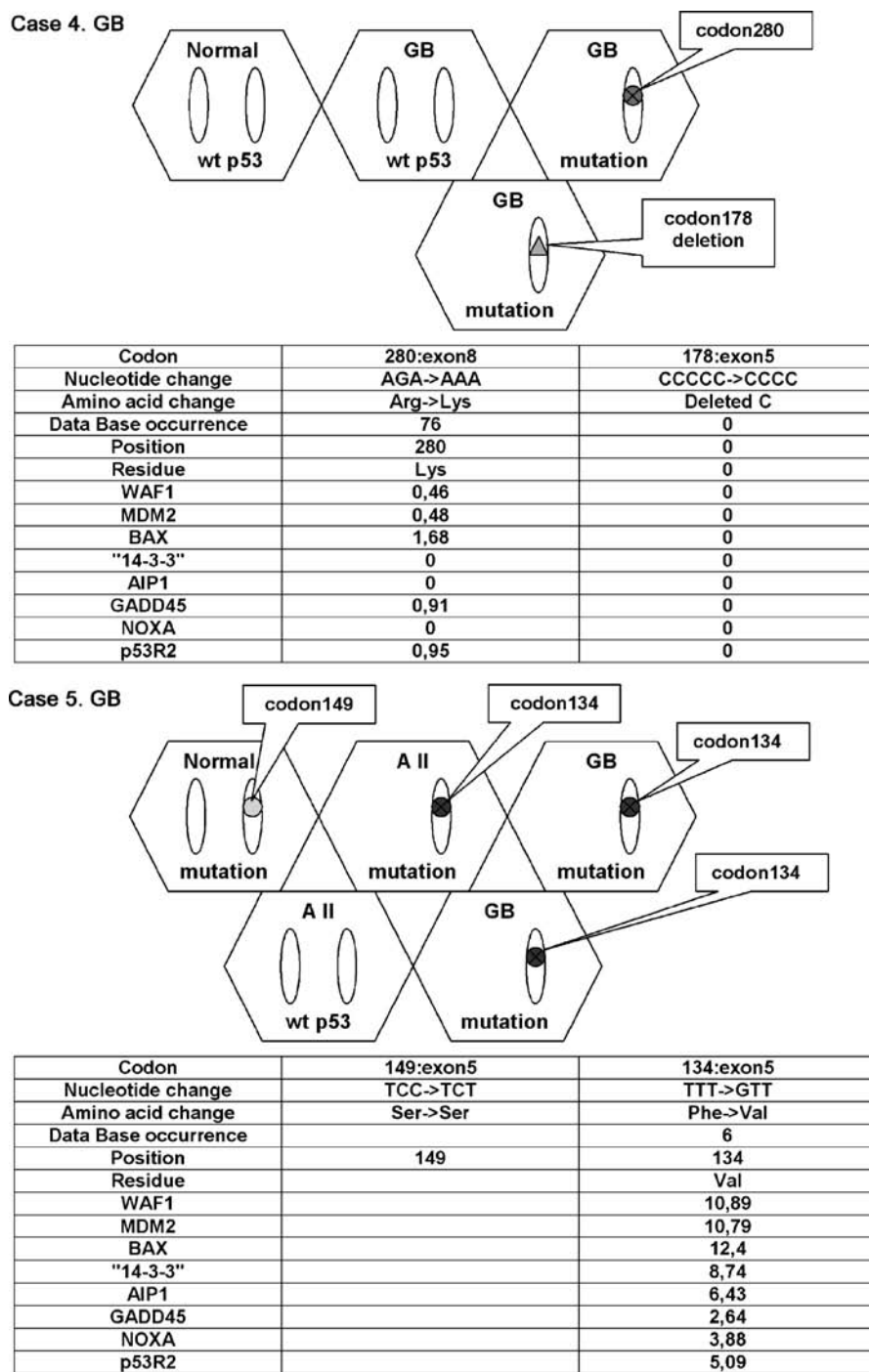
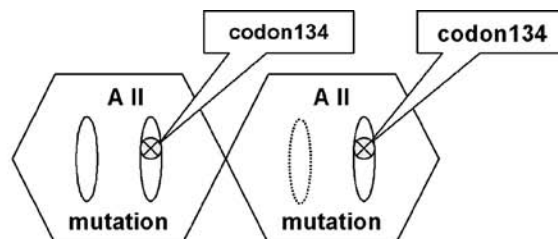


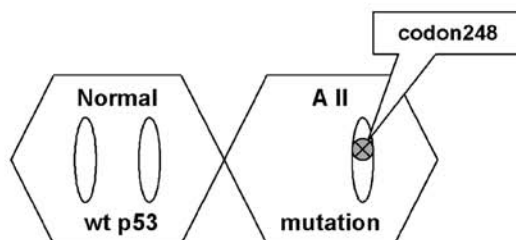
FIGURE 4. Case 4. Glioblastoma (GB). Four areas were dissected including 1 area of normal brain and 3 of GB. Each hexagon represents 1 microdissected cell population. Each unfilled elliptic bar represents 1 p53 allele in the group of cells. The small circle with a cross represents a missense mutation. The small circle without a cross shows a silent mutation. Small triangle represents deletion. One of the 2 mutations found in separate GB areas was a single nucleotide deletion in codon 178 and the other was a missense mutation in codon 280. Both areas with mutations had lost 1 p53 allele. Whether the wild-type (wt) p53 area had both alleles intact or had lost 1 allele could not be determined with the current method. However, we could determine that 3 different molecular changes (2 mutations and loss of 1 allele) were present in tumor areas with similar histopathologic grading. All of these changes have serious consequences in terms of p53 function. Case 5, GB. Five microdissected samples were analyzed. The normal-appearing brain harbored a silent mutation. Interestingly, 3 parts (1 astrocytoma grade II [AII] and 2 GB) of the tumor shared an identical mutation regardless of the difference in tumor grade. The deduced protein had low functional activity, and these 3 cell populations had also lost 1 allele. In another area of AII, there was a wild-type p53 (1 or 2 alleles). This area was morphologically different from the rest with larger, gemistocytic cells (not shown).

Case 9. All



Codon	134:exon5
Nucleotide change	TTT->TCT
Amino acid change	Phe->Ser
Data Base occurrence	2
Position	134
Residue	Ser
WAF1	7,63
MDM2	20,58
BAX	11,19
"14-3-3"	8,64
AIP1	7,02
GADD45	2,89
NOXA	3,5
p53R2	7,17

Case 10. All



Codon	248:exon7
Nucleotide change	CGG->CAG
Amino acid change	Arg->Gln
Data Base occurrence	859
Position	248
Residue	Gln
WAF1	0
MDM2	1,75
BAX	0
"14-3-3"	0
AIP1	0
GADD45	0
NOXA	0
p53R2	0

FIGURE 5. Case 9. Astrocytoma grade II (All). Two areas were microdissected. Each hexagon represents 1 microdissected cell population. Each unfilled elliptic bar represents 1 p53 allele in the group of cells. Small circle with cross represents missense mutation. One identical mutation was found in the 2 morphologically somewhat different All tumor areas. The only difference between the 2 areas was the mutation signal strength. In 1 part of the tumor with lower cell density the wild-type p53 signal was 80%, whereas in the other area it was only about 20%. Because the signal strength could depend on the proportion of normal cells and infiltrating tumor cells in the dissected samples, we hesitate to classify this part as LOH positive. Case 10. All. Two areas were microdissected: normal brain and All. The normal brain displayed wild-type (wt) p53, whereas the All area harbored both a p53 gene mutation and LOH. The codon 248 mutation was a hot spot mutation resulting in a functionally "dead" protein.

interpreted as mutations in the absence of adequate controls. A recent study has shown that a significant number of p53 gene mutations found in the various databases are sequencing errors associated with low-quality DNA (20). To avoid this problem, several controls were included in the present study. First, sequencing has been performed on 2 different PCR

products obtained with 2 different sets of primers. Second, normal DNA obtained from the same paraffin block was also analyzed and, except for 1 case with a silent mutation, no alteration was found in any normal tissue, strengthening the specificity of the mutations found in tumor tissue. Finally, analysis of all these mutations using the UMD p53 database

showed that the identified mutations are not novel and have been previously described in other cancers (see <http://p53.free.fr>).

Histopathologic examination of astrocytic tumors indicates that there is marked intratumoral heterogeneity (see tissue sections) (3, 21, 22). Our study clearly shows that this morphologic heterogeneity is associated with differences at the molecular level as both different and similar mutations of the p53 gene were discovered in morphologically different areas of the same tumor. However, we did not observe a strict correlation between clonal evolution/tumor progression and p53 gene mutational status, as described by earlier studies (23).

We observed that 1 glioma could carry 3 different mutations and that, in a given glioma, 2 areas could at the same time harbor both an identical and 2 different mutations. This was illustrated by case 2, in which 2 different areas of AIII and GB each carried 2 mutations (164 and 234 and 128 and 234), with 1 of these mutations (234) in common. This tumor may have derived from a single cell with a p53 gene mutation in codon 234, especially because this is a hot spot mutation that can provide a growth advantage to cells and thus be selected for. We speculate that this mutation may have occurred at an early stage of tumor development and that some cells subsequently acquired an additional mutation in codon 164 or 128.

On the other hand, findings in case 2 and also in case 5 demonstrate that areas of different grades of malignancy in an astrocytic glioma can share an identical mutation. The results in case 5 also show that both p53 gene mutation and loss of 1 allele are early events in astrocytic glioma, because all 3 parts, including 2 areas of GB and 1 AII area, had 1 mutation in common and all had lost 1 allele. Another part, representing a gemistocytic AII part of the GB tumor, appeared to have a wild-type p53 gene, although we cannot exclude loss of 1 allele. This suggests that there were different molecular genetic pathways involved in the development of this tumor. At the same time, the findings confirm the crucial importance of p53 gene mutations and LOH on chromosome 17p in all grades of astrocytic glioma. Such tumors are associated with deletions of 1 allele but also commonly with mitotic recombination and maintenance of a normal chromosome 17p gene copy number (24).

Hot spot mutations in the p53 gene (found more than 50 times in the database) are known to be fully inactivating and are considered as cancer-driving mutations; however, the situation is less clear for less frequent mutations and more particularly for those found less than 10 times. A high number of these rare mutations display significant transactivational activity. Whether they represent passenger mutations coselected with other cancer-driving mutations (in the p53 gene or any other genes) or mild p53 gene mutations that partially inactivate the p53 protein (leading to certain functional consequences) remains to be determined. In the present study, 2 tumors displayed different functional p53 status in different areas of the tumor (i.e. case 1 with 2 deleterious p53 gene mutations and case 4 with 1 area expressing wild-type p53 and 2 other areas with 2 deleterious p53 gene mutations). These observations reinforce

the notion that different tumor areas evolve independently. Separate development of different tumor areas has been convincingly shown for a human oligoastrocytoma (25).

It has been widely accepted that glioma is a monoclonal neoplasm, also indicated by the p53 gene mutational pattern described in the literature (23, 26–28). However, the opposite opinion also exists, especially concerning multifocal glioblastomas (29–31). In our study, patterns supporting both monoclonal and polyclonal hypotheses were observed. For instance, in cases 1, 4, and 15, different p53 gene mutations existed in different areas of the gliomas, supporting polyclonal events. On the other hand, in cases 2, 5, and 9, an identical p53 gene mutation was found in different microdissected areas, suggesting that these tumors may be of a monoclonal origin. These multiple and seemingly random variations in p53 gene mutation and LOH status within individual glioma tumors illustrate the fact that questions on cell(s) or origin and evolution of astrocytic gliomas need to be addressed by powerful molecular and cell biologic methods to provide valid conclusions.

The fact that such a variable pattern of p53 gene mutations and LOH exists within 1 tumor might not simply reflect tumor progression and does not exclude the possibility that loss of p53 function is an essential driving force in the development of the tumor. Obviously, other abnormalities of the G₁-S transition control genes that lead to deregulation and inactivation of the p14ARF/MDM2/TP53 pathway may have occurred (6). The tendency for multiple p53 gene mutations may reflect some specific pathogenic mechanisms in the subset of astrocytic gliomas that develop p53 gene mutations, for example, related to DNA repair. Nakamura et al (32) described a correlation between MGMT promoter methylation and the presence of p53 gene mutations in low-grade astrocytomas and secondary GBs, with a higher incidence of MGMT promoter methylation in low-grade astrocytomas and secondary GBs with p53 gene mutations.

We found that the mutational status of the p53 gene could vary within a single astrocytic glioma from wild type to several deleterious mutations distributed among areas of different malignancy grade in ways that are difficult to predict. This implies that finding a p53 gene mutation in a small brain biopsy is suggestive of a glioma, but at the same time the absence of p53 gene mutations in a small astrocytic glioma biopsy does not guarantee that the biopsy is from a p53 wild-type tumor.

It is clear that the histologically defined group of GBs represents several molecular subgroups. The current work shows that there are GBs without p53 gene mutations and GBs with mutant p53 gene, in the latter case often with several different mutations and with LOH within the same tumor. Thus, successful treatment of these tumors may require different and individually based therapeutic strategies. Molecular genetic analysis of low-grade and high-grade areas in glioblastomas will help us define new biologically based subgroups of tumors for treatment purpose. This study shows that molecular analysis of the p53 status in the different tumor areas may provide valuable guidance in this process.

ACKNOWLEDGMENTS

We thank Ms. Sha Zhang, Ms. Sofia Vikman, and Ms. Sunna Sigurdardottir at Rudbeck Laboratory, Uppsala University; and Ms. Anna Eriksson at the Department of Oncology Pathology, Karolinska Institutet, for their devoted assistance in this project.

REFERENCES

- Kleihues P, Louis DN, Scheithauer BW, et al. The WHO classification of tumors of the nervous system. *J Neuropathol Exp Neurol* 2002;61: 215–25; discussion 226–29
- Hegi ME, Diserens AC, Gorlia T, et al. MGMT gene silencing and benefit from temozolomide in glioblastoma. *N Engl J Med* 2005;352: 997–1003
- Kleihues P, Cavenee WK. eds. *World Health Organization Classification of Tumours, Pathology and Genetics: Tumours of the Nervous System*. Lyon, France: IARC Press, 2000
- Prados MD, Levin V. Biology and treatment of malignant gliomas. *Semin Oncol* 2000;27:1–10
- Ohgaki H, Kleihues P. Population-based studies on incidence, survival rates, and genetic alterations in astrocytic and oligodendroglial tumors. *J Neuropathol Exp Neurol* 2005;64:479–89
- Ichimura K, Bolin MB, Goike HM, et al. Deregulation of the p14^{ARF}/MDM2/p53 pathway is a prerequisite for human astrocytic gliomas with G₁-S transition control gene abnormalities. *Cancer Res* 2000;60:417–24
- Kato H, Kato S, Kumabe T, et al. Functional evaluation of p53 and PTEN gene mutations in gliomas. *Clin Cancer Res* 2000;6:3937–43
- Okamoto Y, Di Patre PL, Burkhard C, et al. Population-based study on incidence, survival rates, and genetic alterations of low-grade diffuse astrocytomas and oligodendrogliomas. *Acta Neuropathol (Berl)* 2004; 108:49–56
- Walker C, du Plessis DG, Joyce KA, et al. Phenotype versus genotype in gliomas displaying inter- or intratumoral histologic heterogeneity. *Clin Cancer Res* 2003;9:4841–51
- Hedrum A, Ponten F, Ren Z, et al. Sequence-based analysis of the human p53 gene based on microdissection of tumor biopsy samples. *Biotechniques* 1994;17:118–19; 122–24; 126–29
- Ren ZP, Hedrum A, Ponten F, et al. Human epidermal cancer and accompanying precursors have identical p53 mutations different from p53 mutations in adjacent areas of clonally expanded non-neoplastic keratinocytes. *Oncogene* 1996;12:765–73
- Ren ZP, Sallstrom J, Sundstrom C, et al. Recovering DNA and optimizing PCR conditions from microdissected formalin-fixed and paraffin-embedded materials. *Pathobiology* 2000;68:215–17
- Ren ZP, Ahmadian A, Ponten F, et al. Benign clonal keratinocyte patches with p53 mutations show no genetic link to synchronous squamous cell precancer or cancer in human skin. *Am J Pathol* 1997; 150:1791–1803
- Berg C, Hedrum A, Holmberg A, et al. Direct solid-phase sequence analysis of the human p53 gene by use of multiplex polymerase chain reaction and δ -thiotriphosphate nucleotides. *Clin Chem* 1995;41: 1461–66
- Leitner T, Halapi E, Scarlatti G, et al. Analysis of heterogeneous viral populations by direct DNA sequencing. *Biotechniques* 1993;15: 120–27
- Ponten F, Berg C, Ahmadian A, et al. Molecular pathology in basal cell cancer with p53 as a genetic marker. *Oncogene* 1997;15:1059–67
- Hamroun D, Kato S, Ishioka C, et al. The UMD TP53 database and website: Update and revisions. *Hum Mutat* 2006;27:14–20
- Kato S, Han SY, Liu W, et al. Understanding the function-structure and function-mutation relationships of p53 tumor suppressor protein by high-resolution missense mutation analysis. *Proc Natl Acad Sci USA* 2003;100:8424–29
- Soussi T, Kato S, Levy PP, Ishioka C. Reassessment of the TP53 mutation database in human disease by data mining with a library of TP53 missense mutations. *Hum Mutat* 2005;25:6–17
- Soussi T, Asselain B, Hamroun D, et al. Meta-analysis of the p53 mutation base for mutant p53 biological activity reveals a methodological bias in mutation detection. *Clin Cancer Res* 2006;12:62–69
- Burger PC, Kleihues P. Cytologic composition of the untreated glioblastoma with implications for evaluation of needle biopsies. *Cancer* 1989;63:2014–23
- Reifenberger G, Collins VP. Pathology and molecular genetics of astrocytic gliomas. *J Mol Med* 2004;82:656–70
- Sidransky D, Mikkelsen T, Schwechheimer K, et al. Clonal expansion of p53 mutant cells is associated with brain tumour progression. *Nature* 1992;355:846–47
- James CD, Carlom E, Nordenskjold M, et al. Mitotic recombination of chromosome 17 in astrocytomas. *Proc Natl Acad Sci USA* 1989;86: 2858–62
- Coons SW, Johnson PC, Shapiro JR. Cytogenetic and flow cytometry DNA analysis of regional heterogeneity in low grade human glioma. *Cancer Res* 1995;55:1569–77
- Berkman RA, Clark WC, Saxena A, et al. Clonal composition of glioblastoma multiforme. *J Neurosurg* 1992;77:432–37
- Biernat W, Aguzzi A, Sure U, et al. Identical mutations of the p53 tumor suppressor gene in the gliomatous and the sarcomatous components of gliosarcoma suggest a common origin of cells. *J Neuropathol Exp Neurol* 1995;54:651–56
- Kraus JA, Koopmann J, Kaskel P, et al. Shared allelic losses on chromosome 1p and 19q suggest a common origin of oligodendroglioma and oligoastrocytoma. *J Neuropathol Exp Neurol* 1995;54:91–95
- Barnard R, Geddes J. The incidence of multifocal cerebral gliomas: A histological study of large hemisphere sections. *Cancer* 1987;60: 1519–31
- Batzdorf U, Malamud U. The problems of multicentric gliomas. *J Neurosurg* 1963;20:122–36
- Russell D, Rubinstein L, eds. *Pathology of Tumors of the Nervous System*. London, UK: Edward Arnold, 1998
- Nakamura M, Watanabe T, Yonekawa Y, et al. Promoter methylation of the DNA repair gene MGMT in astrocytomas is frequently associated with G:C→A:T mutations of the TP53 tumor suppressor gene. *Carcinogenesis* 2001;22:1715–19